JETIR.ORG ISSN: 2349-5162 | ESTD Year : 2014 | Monthly Issue
JOURNAL OF EMERGING TECHNOLOGIES AND INNOVATIVE RESEARCH (JETIR)
An International Scholarly Open Access, Peer-reviewed, Refereed Journal

Recent Study on Fluorescent Organic Nanoparticles as Chemosensors for Recognition of Metal Ions

Shilpa Y. Salunkhe[1,2*], Dhanaji G. Kanase[2], Suhas S. Mohite[2], Sachin T. Mane[2], Prashant V. Anbhule[3]

1) Department of General Engineering, Bharati Vidyapeeth's College of Engineering, Kolhapur, MS, India.

2) DST-FIST Department of Chemistry, Bharati Vidyapeeth's Dr. Patangrao Kadam Mahavidyalaya, Sangli, MS, India.

3) DST-FIST Department of Chemistry, Shivaji University, Kolhapur, MS, India.

Graphical Abstract:

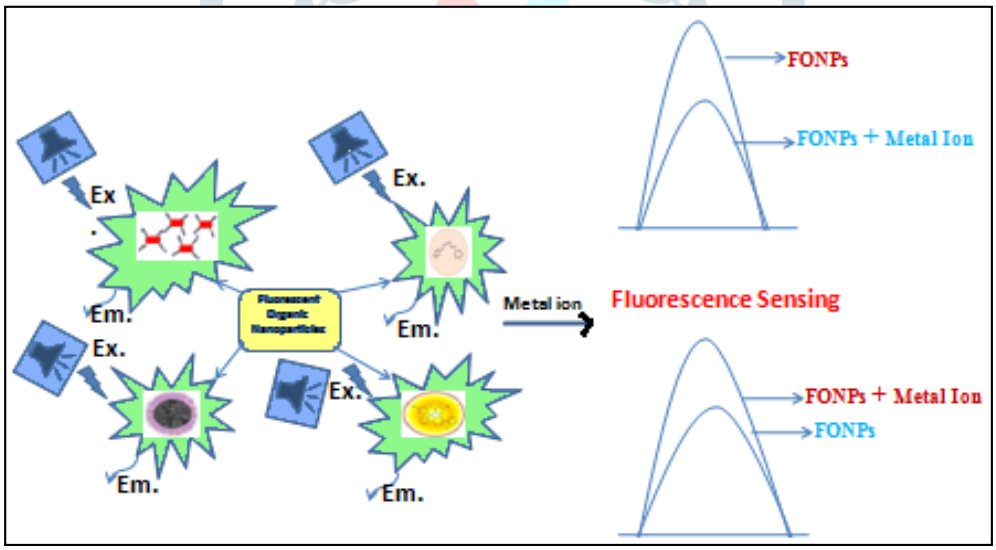

Abstract: Due to their exceptional physico-optical characteristics and simple manufacturing, fluorescent organic nanoparticles (FONPs) have recently gained significant interest in a variety of applications in materials, sensing, biology, and other areas. The π -conjugated small organic compounds have the ability to easily surface modulation and display aggregation induced emission (AIE) property, photo-physical stability, high cytocompatibility, and biodegradability. In this review, we have outlined the fluorescence mechanism, how tiny organic molecules were converted into FONPs, and how FONPs were used as chemosensors to detect metal ions. Different findings indicated a lower detection limit.

Keywords: Chemosensors, Fluorescence mechanism, Fluorescent organic nanoparticles (FONPs), Metal ions.

1. Introduction: The heavy metal ion contamination of aquatic and biological systems is the primary cause of the ongoing rise in environmental pollution [1,2,3]. Supramolecular chemistry research has increasingly focused on designing and developing ion receptors for sensing applications [4,5]. Due to the significance of ions in areas such as environment control, biology, food chemistry, pharmaceutical analysis, and clinical diagnostics, the development of fluorescence-based nanosensor for detection of cations and anions has garnered significant research interest [6–10]. The number of molecular devices that turn physical recordable signals from metal ion sensing is constantly increasing. Fluorescent chemosensors have received a lot of attention recently, and numerous innovative systems have been created. A system that can interact with the metal ion in solution and signal its presence by changing fluorescence properties, such as the wavelength or emission intensity, as well as by the emergence of a new fluorescence band, distinct from those of the free sensor, is considered an effective fluorescent sensor for metal ions.

Several studies have described the detection of metal ions at trace concentrations using conventional analytical techniques, such as surface Plasmon resonance detectors, atomic absorption spectrometry, inductively coupled plasma atomic emission/mass spectroscopy (ICP-AES/ICP-MS), and electrochemical methods [11–16]. These procedures take a long time to prepare samples, need expert workers and expensive, highly sophisticated equipment, and fail to produce selectivity with high sensitivity. In addition to these techniques, fluorescent readout recognition of cations and anions has drawn a lot of interest due to the benefits of fluorescence sensing, which include ease of operation, selectivity, high sensitivity, simplicity, a high degree of specificity, and a low detection limit. Due to its sensitivity and selective behaviour towards a particular analyte, fluorescent organic nanoparticles (FONPs)-based sensors have emerged as a rapidly expanding study area in the field of quantitative analytical chemistry. The selective and sensitive detection of harmful and necessary metal ions from aqueous solutions using FONPs has recently been reported [17–21].

Due to their optical characteristics, FONPs have recently gained a lot of scientific interest. Numerous sensory reports on the creation and synthesis of functionalized FONPs for the detection of metal ions have been published over the last few years [22–26]. Current research is focused on the synthesis of tiny organic molecules for the creation of fluorescent organic nanoparticles in the selective recognition of metal ions. Several techniques, including emulsification evaporation [27], emulsification diffusion [28, 29], laser ablation [28, 29], and reprecipitation method [30] are used to create FONPs. The functionalized fluorescent organic molecule must be more hydrophobic in order for the reprecipitation technique to produce fluorescent nanoparticles, which may then aggregate and form clusters in aqueous media.

The coordination of a metal ion could cause an enhancement of the fluorescence emission, called chelation enhanced fluorescence effect (CEFE) or a quenching of the fluorescence, called chelation enhancement quenching effect (CEQE), both effects can be coupled with a red or blue shift of the emission band. A concise overview of the fluorescence mechanism is presented.

1) Paramagnetic fluorescence quenching: In a variety of metal complexes, a paramagnetic atom (metal ion) is present close to the fluorophore, which causes the formally prohibited intersystem crossover (ISC) to occur more quickly (Fig. 1). The main factor in the d^0 Cu (II) ion's ability to quench fluorescence is a phenomenon known as the paramagnetic effect. Excitation from the S1 to T1 state of the fluorophore, which is thereafter deactivated by bimolecular non-radiative processes, causes ISC in metal complexes containing this metal ion. Due to this, traditional probes for Cu (II) and other strongly paramagnetic metal ions including Fe (III), Cr (III), and Co (II) typically rely on the quenching of fluorescence.

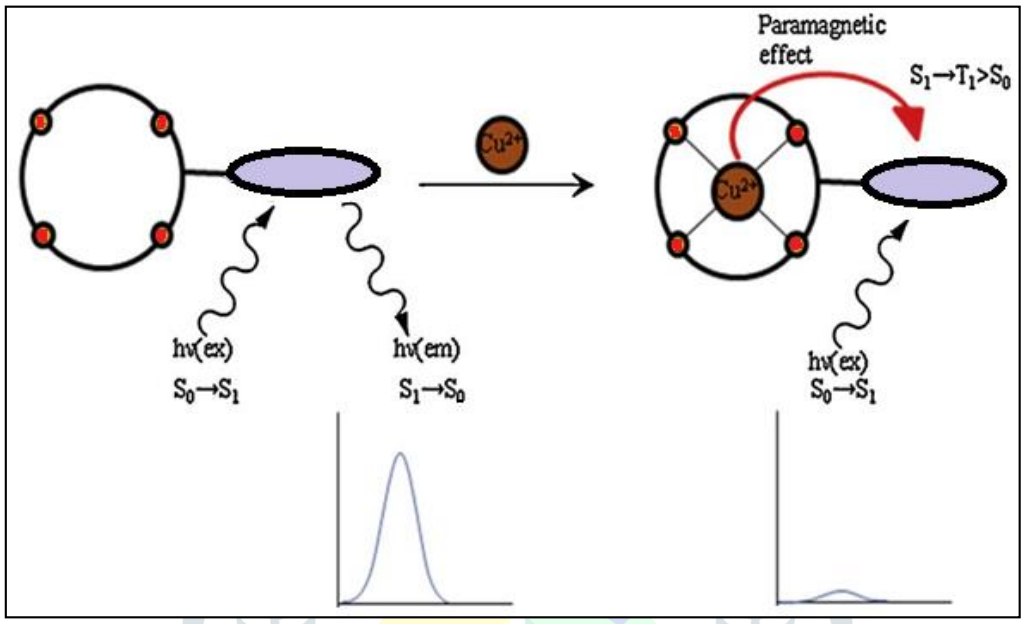

Fig. 1 Paramagnetic Fluorescence Quenching

2) Photoinduced Electron Transfer (PET): PET is a deactivation procedure that involves an internal redox reaction involving a fluorophore in its excited state and a molecule that can provide or take an electron. Consider that the characteristics of the species are significantly different in the excited state compared to the ground-state when trying to understand this process. An excited state is both a stronger reducing and oxidant than the corresponding ground state, especially due to its increased energy content. In fluorescent metal sensors, PET often occurs from a single pair of the coordinating atoms (such as N, O, S, or P) to the excited fluorophore's HOMO (Fig. 2).

The energy of the lone pair involved in the coordination that is inhibiting the PET is reduced when a coordinated metal ion is present, turning on the fluorescence. The oxidation potential of the lone pairs of the coordinating moiety is affected by the solvent polarity, which has a significant impact on PET. The electron transfer is facilitated by higher solvent polarity, which accelerates the Pet-mediated quenching of the fluorescence in high-polar situations.[31–33] Upon complexation of metal ions, the PET type fluorescence response does not result in any spectroscopic change in the emission band.

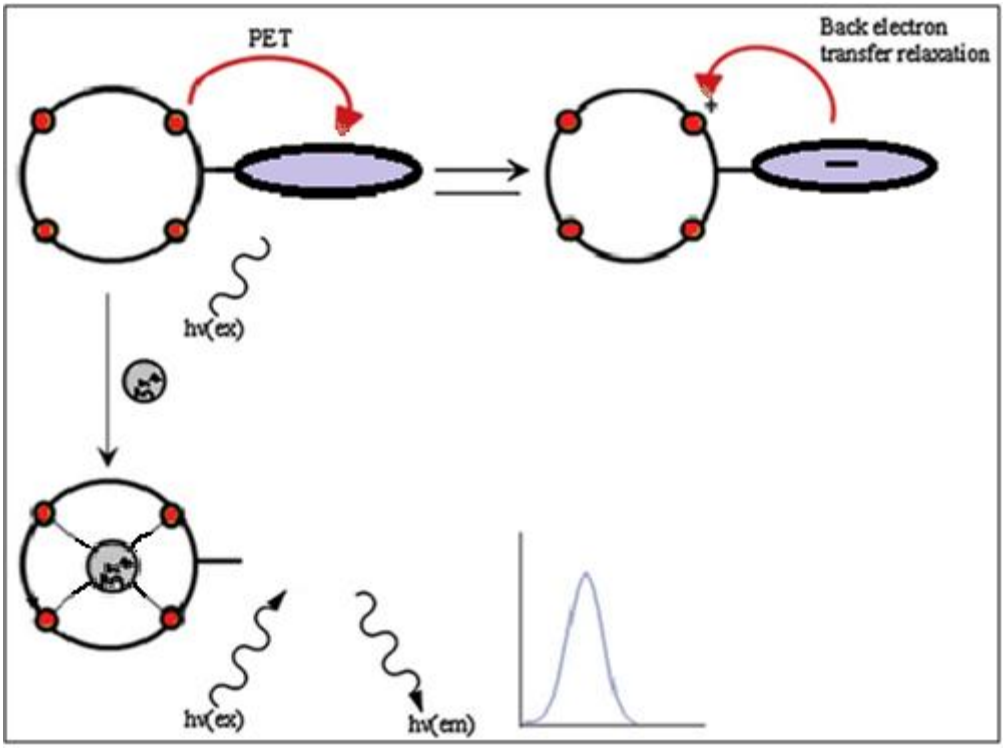

Fig. 2 Photoinduced Electron Transfer

3) Photoinduced Charge Transfer (PCT): In order to promote fluorescence, this method includes the passage of an electron between functions that serve as electron donors and acceptors. A fully conjugated system's has partial charge transfer using PCT sensors. Unlike PET sensors, which have the electron donor moiety separated from the fluorophore by a spacer, all PCT sensors display an integrated receptor and fluorophore. Because of this, depending on the type of fluorophore, metal ion, and complexation mode, the complexation of the metal ion in PCT sensors results in an alteration of electron energy levels that results in a fluorescence turn-OF or turn-ON and a variation in emission and absorption wavelengths (Fig. 3).

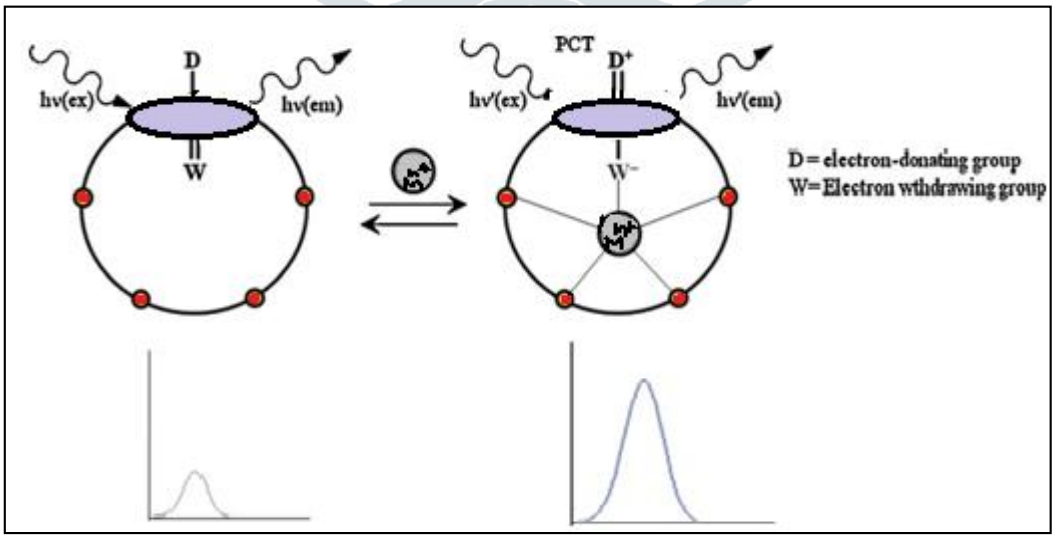

Fig. 3: Photoinduced Charge Transfer

4) Fluorescence Resonance Energy Transfer (FRET): When a fluorophore undergoes FRET, it excites another fluorophore, and the emission of the other fluorophore is detected. FRET is a distance-dependent interaction between the electronic excited states of two fluorophores in which the excitation is transferred from a donor molecule to an acceptor molecule without the emission of photons. FRET must meet the following prerequisites: The donor and acceptor molecules must be close to one another (10–100 A^0 is usual); the acceptor's absorption spectrum must overlap the donor's fluorescence spectrum; and the orientation of the donor and acceptor transition dipoles must be roughly parallel. The inverse sixth power of the intermolecular distance affects FRET efficiency. The two fluorophores are propelled toward or away from one another by the presence of a metal ion. When, free fluorophore A is excited in the first scenario (Fig. 4), FRET cannot occur because of the wide distance between the two fluorophores, therefore the emission spectra of A are observed. By coordinating the metal ion, the gap between the two fluorophores is reduced, activating FRET, which then excites fluorophores A and B, allowing for the detection of their emission spectra [34]. Here, we reviewed the several fluorescent organic nanoparticles (FONPs) that can be used as chemosensors to detect metal ions.

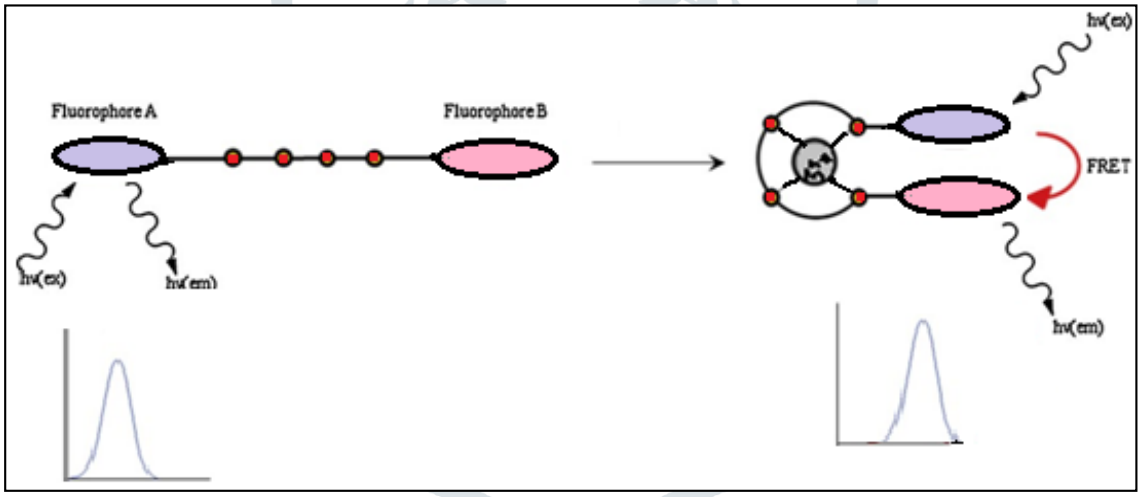

Fig. 4: Fluorescence Resonance Energy Transfer

2. Fluorescent organic nanoparticles (FONPs) as a chemosensors:

2.1. By using the reprecipitation approach, **S. B. Suryawanshi et al.** created surfactant-capped nanoparticles of 9, 10 diphenyl anthracene that were extremely luminous due to aggregation-induced increased emission (AIEE) (Fig. S1). The surfactant cetyltrimethyl ammonium bromide (CTAB) stabilized nanoparticles into brick-shape morphology in addition to producing positive zeta potential on the surface of nanoparticles to attract anions of interest. In comparison to other ions, such as MnO^{2-}, $S_2O_8^{2-}$, HCO_3^-, and $Cr_2O_4^{2-}$, the $Cr_2O_7^{2-}$ ion greatly reduces the fluorescence of nanoparticles. Although the fluorescence of nanoparticles increased in S_2^- and IO_3^-, the interference detected in the Cr (VI) measurement is minuscule. By using methodical fluorescence titration, the selectivity and sensitivity of nanoparticles for recognizing $Cr_2O_7^{2-}$ were investigated. The typical Stern-Volmer

equation can be solved using the fluorescence quenching data. For the estimation of chromium content, a calibration curve is created by graphing quenching of fluorescence (F) versus concentration of Cr (VI), displaying a linear fit in the equation, F = 3070x (x). The quenching data and Cr concentration were found to be linearly correlated, as indicated by the correlation coefficient value R^2 = 0.998, which is almost equivalent to 1. (VI). The method's estimated limit of detection (LOD) values, which are 0.01392 g/mL/1, are far lower than the 0.05 g/mL/1 allowable level of Cr (VI) in drinking water that has been accepted by the World Health Organization (WHO) and the United States Environmental Protection Agency (USEPA). The suggested method of Cr (VI) detection is used on actual samples obtained from a nearby hard chrome deposition company [35].

2.2. The ligand N,N-bis(pyridyl-2-methyl)ethylenediimine (PMEDI) was synthesized by **C. A. Huerta-Aguilar and colleagues**, who subsequently converted it into fluorescent organic nanoparticles (FONPs), which were then examined using analytical techniques (Fig. S2). By monitoring the fluorescence intensity that increased with Zn^{2+} content in the PMEDI solution, the FONPs were used for the precise recognition of Zn^{2+} in an aqueous medium. This demonstrates how PMEDI-FONPs function as chemo-sensors to detect Zn^{2+} in aqueous medium at low concentrations. The Zn^{2+} ion concentration in multivitamin formulations can be detected by this chemo-sensor (FONPs), which can do so selectively for Zn^{2+} in the presence of other nutrient metal ions. Evidently, when the fluorophore is stimulated, photo induced electron transfer (PET) occurs in the PMEDI-FONPs. In the $[PMEDI\text{-}Zn]^{2+}$ system, the creation of a link between the metal ion and the ligand significantly reduces the receptor's HOMO energy, inhibiting PET. The amplification of PMEDI-FONPs' fluorescence emission is caused by the suppression of the PET phenomenon. This is in line with a theoretical study that found that the formation of the $[PMEDI\text{-}Zn]^{2+}$ complex reduces the energy of the ligand's HOMO [36].

2.3. New N_3O_2 macrocyclic ligand (L) was developed by **R. Azadbakht and its co-authors**, and it was examined using spectroscopic methods. The nanoprecipitation process was used to create its nanoparticles. The produced nanoparticles in the optimum circumstances had an average size of roughly 50 nm. In the presence of Al^{3+} ions, the nanoparticles display a "off-on" type mode with great selectivity. Al^{3+} chemosensor in aqueous media could be made from the organic nanoparticles (L). Al^{3+} binds to the nanoparticles, which causes a significant fluorescence enhancement with a turn-on ratio of over 15 times. The nano-chemosensor was not significantly impacted by other metal ions, either. Al^{3+} detection threshold for nanoparticles L was as low as 2.8107 M. The use of the nano-chemosensor (L) as a molecular logic gate has also been investigated [37].

2.4. Rhodamine-based fluorescent nanoparticles were made using a straightforward, speedy, and effective reprecipitation approach by **P. G. Mahajan et al** (Fig. S3). The creation of the required nanoparticles FONPs-RSB as well as its aqueous stability, surface charge, particle size, and morphological aspects were investigated using the characterization techniques such as zeta-particle sizer and scanning electron microscopy. Utilizing absorption and fluorescence experiments, the optical differences between the parent molecule RSB and the FONPs-RSB were investigated. The FONPs-82 RSB's nm particle size and negative zeta potential exhibit a

sphere form. According to the results of the florescence titration, the sphere morphology of FONPs-RSB, which has 82 nm particle size and a negative zeta potential (-33.5 mV), only exhibits sensitive and selective interaction with Hg^{2+} among the series of metal ions examined. Chelation enhanced fluorescence, or CHEF, is a phenomenon that results from the interaction of FONs-RSB with Hg^{2+} and enhances FONs-fluorescence. The fluorescence amplification caused by Hg^{2+} was discovered to be unaffected by the influence of foreign metal ions. Utilizing the Job's and modified Benesi-Hildebrand plots, the binding stoichiometry and binding constant were assessed. Infrared (IR), Nuclear Magnetic Resonance (NMR), absorbance, and fluorescence lifetime titrations in the absence and presence of a varying amount of Hg^{2+} to FONPs-RSB were used to examine the mechanism of binding interaction and nature of complexation. Additionally, mass analysis was used to evaluate the reaction product of the sensing mechanism in the current experiment. According to the calculations made using the current methodology, the detection limits were found to be 1.729 ng/mL (8.619 nM) and 1.68 ng/mL when Hg^{2+} concentration was linear. The additions ranged from 0 to 2 g/mL and from 0 to 100 ng/mL. Utilizing A375 live cells with non-toxic behaviour, the present method's practical application entails the quantitative measurement of Hg^{2+} in ambient samples taken from the nearby campus and intracellular cell imaging of Hg^{2+} [38].

2.5. The sensors were created by **N. Kaur and her co-authors** utilizing silver nanoparticles covered in organic ligands and thoroughly described using spectroscopic techniques. The energy-dispersive X-ray (EDX) examination showed that the surface of metal nanoparticles contained organic receptors. These chemosensors were put to the test in the HEPES buffered DMSO/H2O (8:2, v/v) solvent solution against a variety of biologically and environmentally significant cations. When these chemosensors were coordinated with open shell metal ions like Cu^{2+}/Fe^{3+}, their fluorescence intensity was reduced. The original fluorescence intensity of sensors was recovered upon the addition of phosphate (0–20 mM), and the anion recognition characteristics of the corresponding metal complexes have been examined. As a result, a highly selective chemosensor for the micromolar measurement of phosphate in semi-aqueous medium has been developed [39].

2.6. Brick-shaped 9-Anthraldehyde nanoparticles (9-AANPs) produced by **P. G. Mahajan and colleagues** and coated with cetyltrimethylammonium bromide (CTAB) are visible in a scanning electron microscope image. The average particle size of the nanoparticle suspension, as shown by the Dynamic Light Scattering histogram, is 89 nm. The high level of suspension stability of the nanoparticles is indicated by the positive zeta potential of 20.8 mV recorded on the zeta sizer. The development of H-bonded aggregates via the stacking effect is indicated by the blue shift of 65359.47 cm^{-1} in the UV-Visible absorption spectra of CTAB capped 9-AANPs from the absorption maximum of the dilute solution of 9-Anthraldehyde (9-AA) in acetone. With the addition of phosphate anion solution, the strong Aggregation Induced Enhanced Emission (AIEE) of CTAB capped 9-AANPs at 537 nm is selectively quenched. The results of the nanoparticles fluorescence quenching in aqueous solution fit into the traditional Stern-Volmer relation in the phosphate ion concentration range of 0-40 M. By taking into account the electrostatistically induced phosphate anion adsorption on the positively charged surface

of the nanoparticle produced by the CTAB cap, the potential mechanism of fluorescence quenching of nanoparticles is explicated. On the basis of the fluorescence quenching results of CTAB-capped 9-AANPs, the Langmuir adsorption profile for PO43 adsorption is linear. Within the constraints of the experiments, the estimated values of the Stern-Volmer constant (Ksv) and the Langmuir constant (K) are very similar. Chloroquine phosphate from pharmaceutical tablets is successfully quantified using the phosphate ion sensing approach based on fluorescence quenching of 9-AANPs, allowing the amount of chloroquine to be calculated [40].

2.7. Due to the material's versatility in material production and optical features, **H. Yan et al** reported fluorescent organic nanoparticles (FONPs) have drawn a lot of attention in recent years. A novel Ag^{+} selective turn-on fluorescent chemosensor based on triazolo-thiadiazole (TTD) FONPs was reported in this study (Fig. S4). It exhibits a lowest detectable concentration of 2.87 109 M and significantly enhances the fluorescence of silver ions among fourteen other metal ions. The colloidal solution's fluorescence intensity considerably reduces with the addition of the amino acid cysteine (Cys), which contains thiols, at a limit detection concentration of 2.58 107 M, demonstrating that Cys can form the Ag-Cys complex. As a result, FONPs have the potential to be primary sensors for Ag^{+} and secondary sensors for Cys. The method serves as a foundation for further research on two-component recognition of TTD FONPs. Also addressed is the potential mechanism [41].

2.8. In order to create fluorescein-based organic nanoparticles, **P. G. Mahajan and his co-authors** synthesized N-(3',6'-dihydroxy-3-oxospiro[isoindoline-1,9'-xanthene]-2-yl)-2-hydroxybenzamide (FB) (Fig. S5). By using fluorescence analysis, a series of metal ions' interactions with FB nanoparticles (FBNPs) were studied. When Zn^{2+} ions were added to an aqueous media, FBNPs showed a selective and sensitive fluorescence increase. When FBNPs and Zn^{2+} interacted, chelation enhanced fluorescence was introduced. This effect persisted even after the addition of more metal ions. The UV-visible absorption titration, fluorescence lifespan, and zeta particle size of FBNPs with and without addition of Zn^{2+} all confirmed the establishment of excited state complexation of FBNPs-Zn^{2+}. Results obtained using NMR and IR spectroscopy validated the mode of binding and interaction. The binding constant and stoichiometry calculated using the Job's plot and Benesi-Hildebrand plot, respectively. For Zn^{2+}, the limit of detection (LOD) was 0.0011 g/mL. The remarkable intracellular Zn^{2+} sensor in MDA-MB-231 live cells with minimal toxicity makes the current nano probe (FBNPs) noteworthy. The extraordinary photophysical properties and biocompatibility of FBNPs indicate on-site application of produced fluorescent organic nanoparticles in both the environmental and biomedical fields [42].

2.9. By adopting a straightforward chemical process, **R. Kaur and a coworker** have devised and developed two probes with rhodamine attached thiourea/urea (Fig. S6). The two probes were converted into organic nanoparticles (L1-2), which were hydrophobic by nature and remained stable in aqueous medium. The fluorescence emission from the organic nanoparticles was acceptable and unaffected by the addition of a wide variety of organophosphates. But when evaluated with different cations in buffered aqueous solution, L1 significantly improved with the chromium ion, whereas L2 was non-selective. Additionally, using a cation

displacement assay, the L1.Cr(III) complex detects azinphos methyl specifically even when other organophosphates are present. When azinphos methyl is added to the L1.Cr(III) solution, the fluorescence intensity is modulated, restoring L1's original emission intensity. 1.73 nM is the azinphos methyl detection threshold. Additionally, a metallic sheet that had been precoated with silica was used to detect azinphos methyl. To evaluate the practical application of the sensor, real sample analyses of tap water and river water were conducted [43].

2.10. By using a straightforward reprecipitation technique, **P. G. Mahajan and his co-authors** created the fluorescent N-methyl isatin nanoparticles (N-MINPs) (Fig. S7). With an average particle size of 112 nm, the produced N-MINPs evaluated by dynamic light scattering (DLS) exhibit a narrower particle size distribution. The characteristic spherical form of nanoparticles is visible in the scanning electron microphotograph. When compared to the analogous spectra of the N-methyl isatin solution in acetone, the UV-absorption and fluorescence spectra of the N-MINPs in aqueous suspension are blue shifted. The H-aggregates and Aggregation Induced Enhanced Emission (AIEE) from nanoparticles are indicated by the blue shift. The nanoparticles are highly stable in the absence of any stabilizers, and the functional keto moiety recognized Cd^{2+} ions specifically by increasing the fluorescence preference to Ni^{2+}, Cu^{2+}, Hg^{2+}, Sn^{2+}, Pb^{2+}, Ca^{2+}, Zn^{2+}, Na^{+}, K^{+}, Co^{2+}, and Mg^{2+} ions, which actually appear to quench the fluorescence of the nanoparticles. The investigations on the fluorescence lifespan of N-MINPs and its fluorescence titration with and without Cd^{2+} contributed to the development of a workable theory for how Cd^{2+} enhances the fluorescence of nanoparticles while also improving their ability to attach to other molecules during complexation. On the basis of a chelation-enhanced fluorescence approach, an analytical method for the detection of Cd^{2+} from aqueous medium in environmental samples is further developed using the fluorescence enhancement effect of N-MINPs generated by Cd^{2+} [44].

2.11. According to **G. Kaur et al**, maintaining the body's sodium balance is essential for maintaining normal physiological activities. It is difficult to design a sensitive and selective probe for Na (I) measurement because K (I) ions, in particular, interfere with Na (I) measurements quite obviously. The production of fluorescent organic nanoparticles (ONP) from a Biginelli-based receptor is the foundation of their work. The physiological range of sodium concentration can be measured using the ONP. The sensor exhibits adequate stability in the pH range of 3-11 and for high ionic strength. The competing experiment shows that even in the presence of potentially interfering K (I) ions, the suggested sensor can preferentially detect Na (I). Comparing the projected sensor to other Na (I) sensors described in the literature, its detection limit of 22 nM is pretty excellent. Monitoring Na (I) concentration in biological (urine and sweat samples) and environmental (lake and tap water) samples has also been used to evaluate the probe's practical applicability [45].

2.12. A novel sensor with a mixed imine and amide linkage was created by **S. Chopra and his co-author** using a straightforward condensation procedure between diode amine and catechol carbaldehyde. As these links are typically thought to give receptor design rigidity, they may define the receptor pseudocavity. It is anticipated

that the imine linkages will provide both the binding site and the fluorescent signaling sub-unit. The ligand has been tested for its sensor capabilities in a variety of solvents, and it has demonstrated a strong affinity for Cs^{+}. Fluorescent organic nanoparticles (FONs) of receptor 1igand are created utilizing the re-precipitation process to assess the sensor activity in aqueous media. The AIE phenomenon has been seen by 1igand's FONs in an aqueous solution with an increase in fluorescence intensity at a maximum of wavelength 412 nm. These FONs' fluorescence emission patterns showed modest variations in the low- and high-pH ranges, but they remained stable throughout the pH range of 4–9, making them suitable for usage in environmental/biological studies. As far as we are aware, produced ligand is the first application of FONs as a chemosensor for the nanomolar detection of Cs^{+} in aqueous conditions [46].

2.13. A novel benzothiazole-based chemical was created by **N. Kaur and colleagues**, and it was then used to create fluorescent and redox active organic nanoparticles (1-ONPs) using the nano-re-precipitation process. Dynamic Light Scattering (DLS) and Transmission Electron Microscopy (TEM) methods were used to validate the creation of 1-ONPs, and the size was determined to be 42.84 nm under optimal circumstances. The obtained 1-ONPs performed dual transduction mode Fe^{3+} ion recognition as a selective and sensitive sensor. In the presence of Fe^{3+}, the nanoparticles exhibited a quenching in fluorescence intensity as well as an amplified stripping current response. The current responsiveness of nanoparticles over bulk solution mode was improved by the high surface charge density, and as a result, it is extended to in-field study [47].

2.14. The fluorescent 2-[(E)-(2-phenylhydrazinylidene)methyl]phenol nanoparticles (PHPNPs) were created by **K. S. Patil and his co-authors** using a straightforward reprecipitation technique. With an average particle size of 93.3 nm, the produced PHPNPs evaluated by Dynamic Light Scattering exhibit a smaller particle size distribution. The characteristic spherical form of nanoparticles is visible in the scanning electron microphotograph. In comparison to PHP in acetone solution, the UV-absorption and fluorescence spectra of PHPNPs show a blue shift, indicating H- aggregates and aggregate-induced enhanced emission (AIEE) for nanoparticles. By increasing their preference for fluorescence intensity over Cu^{2+}, Fe^{3+}, Fe^{2+}, Ni^{2+}, NH^{4+}, Ca^{2+}, Pb^{2+}, Hg^{2+}, and Zn^{2+} ions—which actually appear to dampen the fluorescence of nanoparticles—the nanoparticles exhibit a selective inclination towards the recognition of Sn^{2+} ions. The studies on the Sn^{2+}-induced fluorescence enhancement of nanoparticles and their ability to bind during complexation, as well as the Langmuir adsorption plot, fluorescence lifetime of PHPNPs, DLS-Zeta sizer, UV-visible, and fluorescence titration with and without Sn^{2+}, were instrumental in helping to propose a workable mechanism. Further research is done to create an analytical technique for Sn^{2+} detection from aqueous medium in environmental samples using the fluorescence enhancement effect of PHPNPs produced by Sn^{2+} [48].

2.15. Tetrapodal receptor was created by **N. Kaur et al**. and transformed into fluorescent organic nanoparticles (FONs) for the measurement of significant analytes in aqueous medium. With the use of characterization tools, the receptor was completely described. Fluorescence spectroscopy was used to explore the recognition

behaviour of FONs toward various metal ions, and among them, Fe^{3+} ions displayed quenching behaviour in the emission spectra. Tyramine responded ratiometrically to further testing of the Fe^{3+} ion complex of the FONs-based sensor with other biogenic amines. Fluorescence emission profile of FONs'.Fe3+ ion complexes was more useful in biological and environmental samples because they did not vary in pH throughout a wide range. With a detection limit of 377 nM, tyramine detection was linearly proportional to reaction [49].

3. Conclusion:

The review's extensive list of references highlights the development of new fluorescent organic chemosensors that can detect and signal metal ions in solution. This is an active and developing field. Particularly, the field frequently makes use of the already recognized ligand topologies by utilizing their binding characteristics towards particular metal ions. In any event, the foundation of a good chemosensor is the variation of the fluorescent unit by its unique responsive characteristics in terms of wavelength and transduction methods. Because metal ions are frequently insoluble in water, the aqueous media in which they must typically be detected presents a challenge for the application of many fluorescent systems. The expansion of a water soluble fluorescent chemosensor is another goal in the area because the same medium also reduces their fluorescent response, supporting both proton and electron transfer mediated quenching effects.

4. Declaration of Competing Interest:

The authors declared that they have no known competing financial interests or personal relationships that could have appeared to influence the work reported in this paper.

5. Acknowledgements:

Authors greatly acknowledge to D.S.T. New Delhi for sanctioning funds under DST-FIST program to Dr. Patangrao Kadam Mahavidyalaya, Sangli.

4. References:

.

1) Wakshe SB, Dongare PR, Gore AH, Mote GV, Gajare SP, Salunkhe SY, Anbhule PV, Daewon S and Kolekar GB, Env Nano Moni & Mana 2022; 18: 100717.

2) Balaji-Mood M, Naseri K, Tahergorabi Z and Khazdair MR, Fron in Pharmaco 2021; 12: 643972.

3) Briffa J, Sinagra E and Blundell R, Heliyon 2020; 6: e04691.

4) Wakshe SB, Dongare PR, Gore AH, Mote GV, Salunkhe SY, Mahanwar ST, Anbhule PV and Kolekar GB, Inorg Chi Act 2021; 526: 120534.

5) Kaur S, Kaur A, Kaur N and Singh N, Org Biomol Chem 2014; 12: 8230-8238.

6) Eggins BR, Chemical Sensors and Biosensors (Analytical Techniques in the Sciences), John Wiley & Sons Ltd, Chichester, UK, 2002.

7) Basabe-Desmonts L, Reinhoudt DN and Crego-Calama M, Chem Soc Rev 2007; 36: 993.

8) Birkert O, Tunnernann R, Jung G and Gauglitz G, Anal Chem 2002; 74: 834.

9) Ferguson A, Steemers FJ and Walt DR, Anal Chem 2000; 72: 5618.

10) Aylott JW, Analyst 2003; 128: 309.

11) Zhou J, Liu D, He Y, Kong X, Zhang Z, Ren Y, Long L, Huang R and Zheng L, Dalton Trans 2014; 43: 11579.

12) Wei T, Wu G, Shi B, Lin Q, Yao H and Zhang Y, Chin J Chem 2014; 32: 1238.

13) Pohl P and Trend T, Anal Chem 2009; 28: 117.

14) Prestel H, Gahr A, Niessner R and Fresenius J, Anal Chem 2000; 368: 182.

15) Silva EL, Roldan PS and Giné MF, J Hazard Mater 2009; 171: 1133.

16) Khun NW and Liu E, Electrochim Acta 2009; 54: 2890.

17) Mahajan PG, Bhopate DP, Kamble AA, Dalavi DK, Kolekar GB and Patil SR, Anal Methods 2015; 7: 7889.

18) Patil KS, Mahajan PG and Patil SR, Spectrochim. Acta Part A: Mol Biomol Spectro 2017; 170: 131.

19) Mahajan PG, Bhopate DP, Kolekar GB and Patil SR, J Fluoresc 2016; 26: 1467.

20) Bhopate DP, Mahajan PG, Garadkar KM, Kolekar GB and Patil SR, New J Chem 2015; 39: 7086.

21) Dalavi DK, Kamble AA, Bhopate DP, Mahajan PG, Kolekar GB and Patil SR, RSC Adv 2015; 5: 69371.

22) Qu F, Liu J, Yan H, Peng L and Li H, Tetra Lett 2008; 49: 7438–7441.

23) Yan H, Su H, Tian D, Miao F and Li H, Sen Actu B-Chem 2011; 160: 656–661.

24) Hatai J, Pal S and Bandyopadhyay S, RSC Adv 2012; 2: 10941–10947.

25) Wang J, Xu X, Shi L and Li L, *ACS* Appl Mater Inter 2013; 5: 3392 − 3400.

26) An BK, Kwon SK, Jung SD and Park SY, J Am Chem Soc 2002; 124: 14410–1441.

27) Kwon E, Oikawa H, Kasai H and Nakanishi H, Cryst Growth Des 2007; 7: 600–602.

28) Li S, He L, Xiong F, Li Y and Yang G, J Phys Chem B 2004; 108: 10887–10892.

29) Yasukuni R, Hironaka T and Asahi T, J Appl Phys 2010; 49: 06GJ04.

30) Dalavi DK, Bhopate DP, Bagawan AS, Gore AH, Desai NK, Kamble AA, P.G. Mahajan PG, Kolekar GB and Patil SR, Anal Methods 2014; 6: 6948–6955.

31) Czarnik AW (Ed.), Fluorescent Chemosensors for Ion and Molecules Recognition, American Chemical Society, Washington DC, USA, 1993.

32) Balzani V, Campagna S (Eds.), Photochemistry and Photophysics of Coordination Compounds I, Springer-Verlag, Berlin Heidelberg, Germany, 2007.

33) Montalti M, Credi A, Prodi L, Gandolfi MT, Handbook of Photochemistry, third ed., Taylor & Francis Group, Boca Raton, USA, 2006.

34) Formica M, Fusi V, Giorgi L and Micheloni M, Coord Chem Rev 2012; 56: 170–192.

35) Suryawanshi SB, Mahajan PG, Kolekar GB, Bodake AJ and Patil SR, J Phys Org Chem 2018 e3923. https://doi.org/10.1002/poc.3923

36) Huerta-Aguilar CA, Pandiyan T, Raj P, Singh N and Zanell R, Sen and Act B: Chem 2015; http://dx.doi.org/10.1016/j.snb.2015.09.064

37) Azadbakht R, Talebi M, Karimi J and Golbedaghi R, Inorg Chim Act 2016; 453: 728–734.

38) Mahajan PG, Shin JS, Dige NC, Vanjare BD, Han Y, Choi NG, Kim SJ, Seo SY and Lee KH, J of Photochem & Photobio A: Chem **2020** doi: https://doi.org/10.1016/j.jphotochem.2020.112579

39) Kaur N, Kaur S, Kaur A, Saluja P, Sharma H, Saini A, Dhariwal N, Singh A and Singh N, J of Lumin 2014; 145: 175–179.

40) Mahajan PG, Desai NK, Dalavi DK, Bhopate DP, Kolekar GB and Patil SR, J Fluoresc 2014 DOI 10.1007/s10895-014-1451-7.

41) Yan H, Su H, Tian D, Miao F, Li H, Sen and Act B 2011; 160: 656–661.

42) Mahajan PG, Dige NC, Vanjare BD, Han Y, Kim SJ, Hong SK and Lee KH, Sen and Act B: Chem 2018; 119-128

43) Kaur R and Kaur N 2017 doi: 10.1016/j.dyepig.2016.12.032.

44) Mahajan PG, Bhopate DP, Kolekar GB and Patil SR, Sen and Act B 2015; 220: 864–872.

45) Kaur G and Kaur N, Sen and Act B: Chem 2018; 265: 134-141.

46) Chopra S, Singh N, Thangarasu P, Bhardwaj VK and Kaur N, Dyes and Pig 2014; 106: 45-50.

47) Kaur N, Kaur R, Kaur R and Rana S, Inorg Che Comm 2021; 129: 10864.

48) Patil KS, Mahajan PG and Patil SR, Spectrochem Acta Part A: Mol and Biomol Spectro 2017; 170: 131–137.

49) Kaur N, Kaur M, Chopra S, Kuwar A and N Singh, Food Chemistry 2018; 245: 1257-1261.